Published in final edited form as:
Cancer Res. 2011 July 1; 71(13): 4675–4685. doi:10.1158/0008-5472.CAN-10-4558.

Perinatal or adult *Nf1* inactivation using tamoxifen-inducible *PlpCre* each cause neurofibroma formation

Debra A. Mayes[1], **Tilat A. Rizvi**[1], **Jose A. Cancelas**[1,3], **Nathan T. Kolasinski**[1], **Georgianne M. Ciraolo**[2], **Anat O. Stemmer-Rachamimov**[4], and **Nancy Ratner**[1]

[1]Experimental Hematology and Cancer Biology, Cincinnati Children's Hospital Medical Center

[2]Pathology, Cincinnati Children's Hospital Medical Center

[3]Hoxworth Blood Center, University of Cincinnati

[4]Department of Pathology, Massachusetts General Hospital and Harvard Medical School

Abstract

Plexiform neurofibromas are peripheral nerve sheath tumors initiated by biallelic mutation of the NF1 tumor suppressor gene in the Schwann cell lineage. To understand whether neurofibroma formation is possible after birth, we induced *Nf1* loss of function with an inducible proteolipid protein Cre allele. Perinatal loss of *Nf1* resulted in the development of small plexiform neurofibromas late in life, while loss in adulthood caused large plexiform neurofibromas and morbidity beginning 4 months after onset of *Nf1* loss. A conditional EGFP reporter allele identified cells showing recombination, including peripheral ganglia satellite cells, peripheral nerve S100β+ myelinating Schwann cells, and peripheral nerve p75+ cells. Neurofibromas contained cells with Remak bundle disruption but no recombination within GFAP+ non-myelinating Schwann cells. Extramedullary lympho-hematopoietic expansion was also observed in *PlpCre;Nf1fl/fl* mice. These tumors contained EGFP+/Sca-1+ stromal cells among EGFP-negative lympho-hematopoietic cells indicating a non-cell autonomous effect and unveiling a role of Nf1-deleted microenvironment on lympho-hematopoietic proliferation in vivo. Together these findings define a tumor suppressor role for *Nf1* in the adult and narrow the range of potential neurofibroma-initiating cell populations.

Keywords

Neurofibromatosis type 1; Neurofibroma; satellite cell; Schwann cell; lymphoma

Introduction

Neurofibromatosis type 1 (NF1) is an autosomal dominant inherited disease, affecting approximately 1:3000 individuals worldwide (1). Disease manifestations are observed after mutation or loss of *NF1* in diverse cells and tissues. Common findings include learning and memory difficulties, and optic pathway gliomas (2-3). Rarer manifestations include juvenile myelomonocytic leukemia (JMML) (4-6), a myelodysplastic/myeloproliferative neoplasm characterized by monocytosis, lymphadenopathy and hepatosplenomegaly.

Most NF1 patients (>90%) develop tumors within the peripheral ganglia, peripheral and/or cranial nerves called neurofibromas, composed of cell types including neuronal axons, fibroblasts, perineurial cells, Schwann cells, and mast cells (7). Homozygous loss of *NF1* is

Author for correspondence: Nancy Ratner: Tel: (513)-636-9469, Fax: (513)-636-1083, nancy.ratner@cchmc.org.

present only within the Schwann cell compartment (8-10) indicating that cells within the Schwann cell lineage are necessary for neurofibroma formation. In humans, plexiform neurofibromas can be congenital, suggesting a possible role for a developing Schwann cell in neurofibroma formation. However, the cell(s) of origin for neurofibroma formation within the Schwann cell lineage remain unclear.

Neural crest cells develop into Schwann cell precursors between E11 and E13 in mouse sciatic nerve, and Schwann cells by E18 (11-12). Progenitors identified after the establishment of the dorsal root ganglia (DRG) have more limited self-renewal and differentiation potential than neural crest stem cells (13-17). Schwann cells differentiate in close association with the axons of peripheral nerves. Those Schwann cells associated with neuronal cell bodies form satellite cells that express either S100β or GFAP. Schwann cells ensheathing multiple small axons in peripheral nerves are GFAP+ non-myelinating Schwann cells, while Schwann cells associating with single large axons form myelin and express S100β and periaxin (18). Neurofibroma initiating cells may be committed glial cells, de-differentiated Schwann cells, and/or post-crest progenitor cells.

Nf1−/− mouse embryos die by E13.5 due to abnormal heart development and *Nf1+/−*mice do not develop neurofibromas (19-20). Loss of *Nf1* in animal models using neural crest drivers Wnt1-Cre (E9.5), Mpz-Cre (E9.5-10.5), and Pax3-Cre (E10.5) did not result in neurofibroma formation (21). These findings suggested that a post-crest target cell(s) drives neurofibroma formation; therefore, several laboratories targeted *Nf1* loss to Schwann cell populations after neural crest migration. In a pioneering study a Krox20-Cre driver line, which expresses within boundary cap cells at E10.5 and later in Schwann cells in peripheral nerves, caused GEM neurofibroma formation (22). A $P0_A$-Cre+ driver line in which loss of *Nf1* begins in neural crest at E9.5 with robust expression at E12.5 also enabled neurofibroma formation (23). Loss of *Nf1* in embryonic Schwann cells (E12.5) also caused neurofibroma formation (24). Thus cell(s) developing at or after the embryonic Schwann cell stage of development initiate neurofibroma formation.

Peripheral nerve Remak bundles containing small diameter axons ensheathed by a single Schwann cell are disrupted in all neurofibroma models. In contrast, myelinated axons appear relatively spared. This led to the suggestion that non-myelinating Schwann cell are tumor-initiating cells within neurofibromas (23).

Myelin proteolipid protein (Plp) is a component of the Schwann cell myelin sheath (25). We used a tamoxifen-inducible *PlpCre* driver line (Plp-Cre-ERT [designated *PlpCre* throughout]) to test the potential role of *Nf1* loss within Plp-expressing cells in neurofibroma formation (26), inducing *Nf1* loss after birth or in adult animals. We report that *Nf1* inactivation at either age results in neurofibroma formation. While Remak bundle disruption is shown within the neurofibromas, GFAP+ non-myelinating Schwann cells do not show *Nf1* inactivation.

Materials and Methods

Mouse husbandry

Cincinnati Children's Hospital Research Foundation animal care and use committee approved all animal use. Mice were housed in a temperature- and humidity-controlled vivarium on a 12 hour light-dark cycle with free access to food and water.

Mouse Strains

Nf1 flox/+ mice on a mixed 129/Bl/6 background (22) were mated to female tamoxifen-inducible *PlpCre* C57Bl6 mice (26). *PlpCre;Nf1fl/+* mice were bred to mice containing a

CMV-β actin loxP flanked CAT gene upstream of the enhanced green fluorescent protein cassette (27).

Perinatal Tamoxifen Injections

Tamoxifen (100mg) was dissolved in 1ml of ethanol and 9mls of sunflower seed oil. Intraperitoneal (I.P.) tamoxifen injection (1mg/100ul) was twice a day for 3 consecutive days to lactating mothers, administering tamoxifen to pups through the mother's milk, beginning when pups were 1 day old. Dose-limiting toxicity was pup trembling and occasional mortality, when tamoxifen was provided twice a day for >3 days. Tamoxifen injection once-daily for 3 or 5 days to the mother failed to cause peripheral nerve recombination.

Adult Tamoxifen Injections

100ul (1mg/100ul) was administered I.P. once or twice a day for 3 consecutive days. Tamoxifen administration once daily for 3 or 5 consecutive days did not result in significant adult peripheral nerve recombination. We dosed twice a day for 3 consecutive days.

Genotyping and Recombination and survival studies

Mice were genotyped by PCR (22, 26, 27). *Nf1* recombination was determined 30 days after tamoxifen injections using PCR (22). *PlpCre;Nf1fl/fl* mice were euthanized when they became paralyzed, failed to groom, had obvious weight loss, or developed tumor masses.

Tissue processing

We administered Brdu I.P. (50 mg/kg body weight) 3 times at 2 hour intervals. Two hours later, we anesthetized mie and perfused with ice cold 4% paraformaldehyde. Tissues were removed and photographed on a Leica MZFL111 microscope, then post-fixed in 4% paraformaldehyde overnight for paraffin sectioning or for an hour with transfer to 20% sucrose for frozen sectioning. For electron microscopy, we perfused mice with 4% paraformaldehyde and 2.5% glutaradehyde, post–fixed in the same fixative overnight, and then transferred tissues to 0.175M cacodylate buffer, osmicated, dehydrated and embedded in Embed 812 (Ladd Research Industries, Burlington, VT). Ultrathin sections were stained in uranyl acetate and lead citrate and viewed on a Hitachi Model H-7600 microscope.

Histology

Paraffin sections were processed for H&E to examine tissue structure or stained with Toludine Blue to identify mast cells. An *in vitro* Brdu staining kit monitored proliferation (Invitrogen, Carisbad, CA). Biotinylated secondary antibodies were used at 1:200 (Vector), together with an ABC kit to visualize immunoreactivity (Vector Labs, Burlingame, CA).

Antibodies

Cryostat sections were air dried and processed for immunohistochemistry using markers for EGFP (chicken GFP 1:2000; Millipore, San Diego, CA), myelinating Schwann cells (rabbit S100β 1:25,000 for fluorescence and 1:30,000 for DAB; DAKO, Carpinteria, CA), non-myelinating Schwann cells (rabbit GFAP 1:500; DAKO, Carpinteria, CA), Schwann cells with glutathione synthase (rabbit GS 1:250; Santa Cruz Biotech, Santa Cruz, CA), mesenchymal cells (Sca-1 1:200; clone D7, BD-Pharmingen, San Jose, CA). Fluorescent secondary antibodies were used at 1:200 (Jackson Immuno Labs, West Grove, PA) except for Alexa 594 at 1:800 (rabbit or mouse; Invitrogen, Carisbad, CA). Histomount or Fluoromount G was used to coverslip DAB or fluorescent sections, respectively. Fluorescent images were captured on a Zeiss Axiovert 200M microscope using a 40× Plan-NEO FLUAR objective, Hamumamatsu Orca ER camera, and ImageJ software.

Complete Blood Counts and Flow Cytometry Analysis

Peripheral blood counts were performed in a Hemavet counter (Drew Scientific, Waterbury CT). Blood smears were stained with Diff-Quick for manual counts. Flow cytometry analysis used CD45R/B-220 (clone RA3-6B2)-Pacific Blue, CD3e (clone 145-2C11)-PerCP-Cy5.5, Mac-1 (CD11b, clone M1/70)-PE, Gr-1/Ly6C-G (RB6-8C5)-APC-Cy7 and CD117 (ACK45)-APC (Becton Dickinson, San Jose, CA) and analyzed for co-expression of EGFP on an alive gate selected based on light scatter parameters in a FACS Canto flow cytometer (Becton Dickinson).

Statistical Analyses

Kaplan Meier survival curves were created using GraphPad Prism software and Log-rank Mantel-Cox Tests. Counting of Schwann cells and satellite cells was performed on at least 150-300 EGFP+ cells per area per animal from 3-5 animals per genotype. Two-way *t*-tests were performed on CBC X Blood Smear counts and immuno-reactive cell counts with a significance cutoff of $p<0.05$.

Results

Postnatal (P1-3) loss of *Nf1* in *PlpCre;Nf1fl/fl* mice causes early and later mortality

To test whether loss of *Nf1* within postnatal cells elicits tumors *in vivo*, we chose a tamoxifen-inducible *PlpCre* driver. Survival was monitored after postnatal (1-3) tamoxifen exposure within *PlpCre* mice and showed two phases of mortality (Figure 1A; $p < 0.0001$). Seven of 36 *PlpCre;Nf1fl/fl* animals died when they were 5-7 months old, displaying hematopoietic lesions characteristic of lymphoma (7/36 = 20%; Supplemental Table 1). No neurofibroma formation was observed upon gross dissection of these 7 mice.

The remaining *PlpCre;Nf1fl/fl* animals (29/36; 80%) required sacrifice at 15 – 21 months of age. Littermate *PlpCre;Nf1wt* controls (designated “WT controls” or wild type throughout the manuscript) remained healthy. On gross dissection these *PlpCre;Nf1fl/fl* animals had enlarged peripheral nerves associated with paraspinal tumors at cervical (Figure 1B) and thoracic spinal levels. Sixty-seven percent (4/6) of mice in which full neuroaxis dissection was performed also had paraspinal tumors within the lumbar/sacral regions (Supplemental Table 1). Grading and classification of tumors used GEM nerve sheath classification (28). GEM neurofibromas Grade I are defined as tumors with histological features similar to those of human neurofibromas; hypocellular with abundant matrix and collagen fibers, minimal cell atypia and rare mitosis. There are often intermixed nerve axons and mast cells present. All paraspinal tumors in the *PlpCre;Nf1fl/fl model* were GEM Grade I neurofibromas. On histological analysis, they showed low cellularity, stromal matrix between the cells, S100β+ myelinating Schwann cells, and mast cell infiltration (Figure 1C).

PNST formation after perinatal or adult tamoxifen exposure in *PLPCre;Nf1fl/fl* mice

One in 5 *PlpCre;Nf1fl/fl* mice developed GEM Grade III PNST (Supplemental Table 1 and Supplemental Figure 1). Similar to human MPNSTs, GEM Grade III PNST are densely cellular tumors with marked anaplasia, high nuclear/cytoplasmic ratio, and frequent mitoses (Supplemental Figure 1A-C, right). Tumors arose in the abdomen, at the base of the tail, or in hindlimbs after either perinatal or adult loss of *Nf1*. Clear relationships to lower grade neurofibroma and/or proximity to S100+ cells enabled classification as GEM PNST (Supplemental Figure 1A, right insert).

Perinatal Tamoxifen exposure in *PlpCre;Nf1fl/fl* mice causes reactive hyperplasia of hematopoietic cells

Endogenous Plp is expressed in spleen and thymus as well as glial cells (29). Therefore, this *PlpCre* driver could be expressed within hematopoietic cell populations. Postnatal (P1-3) tamoxifen injections within *PlpCre;Nf1fl/fl* animals caused development of tumors resulting from extramedullary expansion of lymphoid and myeloid cell populations in 36% of the animals examined. Seven developed early (by 5-7 months of age) and 7 animals contained hematopoietic-containing tumors at necropsy in the context of complications arisen from neurofibroma formation (15-22 months of age). Enlarged organs with solid white lesions were noted within the liver, spleen, lung, kidney, lacrimal gland, and lymph nodes within the abdominal cavity, neck, inguinal and axillary regions (Figure 2A). Within the subset of animals that developed these tumors, splenomegaly, a prominent finding in a number of hematopoietic abnormalities including JMML, was common (Figure 2A, right). These animals often suffered dermatitis of the face and neck. While eczema is common in JMML, these dermal lesions overlaid neurofibromas deep within the tissue.

To characterize the hematopoietic lineage within these tumors, flow cytometry analysis of splenocytes or abdominal masses from *PlpCre;Nf1fl/fl;EGFP+* mice was performed. Tumors were composed of a heterogeneous hematopoietic cell population (B cells, T cells and myeloid cells), which were EGFP negative (Figure 2B). We examined the peripheral blood of wild type and *PlpCre;Nf1fl/fl* animals at 7 months of age. Total CBC and Blood Smear Counts showed an increase in polymorphic mononuclear cells (PMN; $p = 0.0026$) and lymphocytes (LY; $p = 0.0006$), with a decrease in monocytes (MO; $p = 0.0347$) in *PLPCre;Nf1fl/fl* animals compared to age-matched littermate controls (Figure 2C).

Histological analysis of tumor sections revealed the presence of EGFP+ cells morphologically distinct from the lympho-myeloid infiltrate (Figures 2D). EGFP+ cells were spindle shaped, infiltrated the lymphohematopoietic tissue and some EGFP+ cells expressed Sca-1, a recognized marker of mesenchymal cells and progenitors with hematopoietic supportive ability in C57Bl/6 and FVB/N background mice (30-32) (Figure 2D). Flow cytometry studies of adult *PlpCre* blood and bone marrow confirmed the absence of EGFP+ within progenitor and mature hematopoietic cells (data not shown). These data indicate that loss of *Nf1* within this model causes an unidentified hematopoietic proliferative disorder distinctive from JMML. Furthermore, because EGFP+ recombination did not occur within hematopoietic-lineage cells, cell hyperproliferation occurs in a non-cell autonomous fashion after perinatal (P1-3) loss of *Nf1* within *PlpCre*+ non-hematopoietic, stromal cells.

Adult loss of *Nf1* can cause neurofibroma formation

To test whether loss of *Nf1* within adult animals can elicit tumor phenotype(s) *in vivo*, we injected adult (8 – 10 week) *PlpCre;Nf1fl/fl* mice with tamoxifen. All mutant mice required sacrifice between 7 and 15 months of age (5-13 months post tamoxifen exposure) due to paralysis, while littermate *WT* controls remained healthy (Figure 3A; $p < 0.0001$). Hematopoietic tumors were evident in 3/20 (15%) of adult tamoxifen-injected *PlpCre;Nf1fl/fl* animals on gross dissection.

Gross dissections were performed on the neuroaxis of 20 *PlpCre;Nf1fl/fl* animals. All had tumors associated with peripheral nerves and DRGs (Supplemental Table 1), and cranial-facial nerves. Figure 3B displays representative tumors associated with spinal and peripheral nerves of a *PlpCre;Nf1fl/fl* animal, diagnosed as GEM Grade I neurofibromas after paraffin embedding and staining with H&E (Figure 3C). Similar to perinatal *PlpCre;Nf1fl/fl* neurofibromas, these displayed low cellularity with increased stroma between the cells. The neurofibromas contained characteristic S100β+ cells and mast cell infiltration (Figure 3C).

Recombination was examined by PCR analysis (Figure 3D). As expected, recombination was noted within the brain and peripheral nervous system (sciatic nerve & dorsal root ganglia). Recombination was also detected in the heart, lung, spleen, thyroid, skin, fat and bone. Recombination was absent within the liver, kidney, and bone marrow. EGFP+ cells were present within peripheral nerves throughout the body (data not shown). Organ-specific EGFP+ cells were also noted within the heart, lung, thyroid, and spleen (Supplemental Figure 2), likely accounting for some of the recombination observed.

Comparison of neurofibroma formation after perinatal or adult tamoxifen exposure in *PlpCre;Nf1fl/fl* mice

When compared to 15 month old wild type controls (Figure 4A), *PlpCre* animals after either perinatal (Figure 4B) or adult (Figure 4C) loss of *Nf1* show neurofibroma formation in cranial nerves (Figure 4, top panel), DRGs, and peripheral nerves (Figure 4B & 4C). Cranial nerves commonly developed neurofibromas extending into the face, neck and tongue. These tumors sometimes compressed the brainstem, which resulted in head tilt and circling behavior (Figure 4B asterisks). Neurofibromas were larger in mice injected with tamoxifen as adults, likely accounting for earlier animal lethality. Some tumors compressed the spinal cord; however, commonly tumors surrounded the DRG and extended laterally along peripheral nerves. *PlpCre;Nf1fl/fl* cauda equina nerves also showed enlargement and nerves often showed kinks (Figure 4D).

Remak bundle disruption within *PlpCre;Nf1fl/fl* Saphenous Nerves

Electron microscopy compared saphenous nerves of 12 month old *PlpCre+;Nf1wt* control (Figure 5A), postnatal (P1-3) tamoxifen-injected *PlpCre+;Nf1fl/fl* (Figure 5B), and adult tamoxifen-injected *PlpCre+;Nf1fl/fl* animals (Figure 5C) to determine whether loss of *Nf1* within *PlpCre*+ cells affects Remak bundles. Similar to other mouse neurofibroma models, myelination of large diameter axons appeared normal after either perinatal or adult loss of *Nf1* while perinatal or adult tamoxifen exposure caused Remak bundle disruption (Figure 5B & C). Thus many small caliber axons were found in a one to one relationship with an attendant axon while other Schwann cells were dissociated from axons completely, and pathologically wrapped collagen.

PlpCre targets multiple glial cell types in the peripheral nervous system: identification using EGFP

To define cells targeted by the *PlpCre* driver, we analyzed *PlpCre; CMB-β actin loxP EGFP* flanked CAT mice one day post last tamoxifen injection (i.e. 4 days post tamoxifen introduction). The percent of EGFP+; DAPI+ non-neuronal cells was higher in DRG and sciatic nerve after perinatal injection compared to adult tamoxifen injection (Figure 6A left). The development of immature Schwann cells into myelinating and non-myelinating nerve Schwann cells is incomplete in perinatal life (12). Therefore we focused on defining cell types expressing *PlpCre* (EGFP+ staining) in adult mice. EGFP was detected in 7% of the non-neuronal cells within cervical DRG and 18% of cells within the adult sciatic nerve. The percentage of EGFP+;S100β+ satellite cells in the DRG was 11%; and myelinating Schwann cells in sciatic nerve = 25% (Figure 6A right, & 6B). S100β+ cells in the sciatic nerve were myelinating Schwann cells as confirmed by double labeling with anti-periaxin (data not shown). In neurofibromas, months after tamoxifen exposure *PlpCre;Nf1fl/fl* cells continue to show EGFP double labeling with S100β+ (Figure 6B).

In wild type mice, the percentage of double-labeled EGFP+;GFAP+ cells 4 days after tamoxifen within the DRG was 34%; and sciatic nerve = 0% (Figure 6A right, & 6C). Thus, the *PlpCre* construct is not active within the GFAP+ non-myelinating cells in the peripheral

nerve. In neurofibromas, months after tamoxifen exposure *PlpCre;Nf1fl/fl* cells did not express GFAP (Figure 6C).

There were no EGFP+;p75+ wild type satellite cells within the DRG 4 days after tamoxifen (Figure 6D). EGFP+;p75+ cells were present in the sciatic nerve (Figure 6D). EGFP+ cells (59% in DRG, & 41% in sciatic nerve) double-labeled with the Schwann cell and satellite cell marker glutathione synthase (GS) (Figure 6A right). Thus the *PlpCre* driver targets myelinating S100β+ Schwann cells within the sciatic nerve, and unidentified p75+ cells. Within the DRG, all EGFP+ cells had the morphology of satellite cells, with distinctive cell processes wrapping around DRG neurons.

Rapid onset of proliferation in *Nf1* mutant cells

We noted that the numbers of EGFP+ cells in *PlpCre;Nf1fl/fl* dorsal root ganglia appeared to increase over time (Figure 7A). Quantification of EGFP+ cells at 1, 7, and 28 days following tamoxifen injection in the sciatic nerve showed that beginning 1 day after the final tamoxifen injection the numbers of EGFP+ cells were significantly increased in *PlpCre;Nf1fl/fl* as compared to wild type (Figure 7B). We monitored cells in the S-phase of the cell cycle with BrdU immunostaining. Many nerve and neurofibroma EGFP+ cells were BrdU+, likely accounting at least in part for the observed increase in cell number (Figure 7C).

Discussion

In this study we found that both postnatal (P1-3) and adult loss of *Nf1* using the *PlpCre* driver cause GEM-grade I neurofibroma tumor formation. The models differ in the timing of neurofibroma formation, in the size of the neurofibromas generated, and in prevalence of hematopoietic manifestations. We found that myelinating Schwann cells, p75+ cells, and satellite cells are targeted by the inducible *PlpCre* driver. Our results support previous studies indicating that loss of *Nf1* in subpopulations of nerve Schwann cell lineage cells cause neurofibroma formation, and extend these studies by showing that acute *Nf1* loss, after organogenesis and cell differentiation, can be tumorigenic.

We identified EGFP+ cells in order to identify possible tumor cells of origin in the *PlpCre* model. Tamoxifen exposure induced peripheral nervous system recombination, as judged by EGFP+ cells, in satellite cells in the DRG (S100β+ or GFAP+) with the characteristic morphology of satellite cells, closely wrapping DRG cell bodies. In *DhhCre;Nflfl/fl* mice, satellite cells do not show recombination, yet neurofibromas form (24). While not definitive, the combination of the two models does not support a role for satellite cells in mouse neurofibroma formation; however, the possibility that satellite cells are important for neurofibroma formation in some settings while not in others cannot be excluded.

Most EGFP+ cells in adult peripheral nerves were S100β+ (myelinating) Schwann cells. This result is expected, as endogenous Plp is a characteristic of myelinating Schwann cells in adult peripheral nerve (33). At the EM level, *Nf1* loss did not dramatically alter myelination.

Remak bundle disruption is a characteristic feature of all neurofibroma models (22-24, 34). When the non-myelinated Schwann cell population was examined, no EGFP+;GFAP+ non-myelinating Schwann cells were identified. These data are surprising as electron microscopy shows disruption of the association between axons and non-myelinating Schwann cells in the *PlpCre;Nf1fl/fl* model. We conclude that *Nf1* loss within GFAP+ cells is not necessary for Remak bundle disruption in the *PlpCre;Nf1fl/fl* model.

We identified EGFP+;p75+ cells in peripheral nerve. These may be a sub-population of GFAP-negative non-myelinating cells, and/or an as-yet unidentified population(s) in adult peripheral nerve. Zheng et al. (2008) proposed that the p75+ non-myelinating cell population was the cell of origin for neurofibroma formation (23). The present study eliminates the GFAP+ non-myelinating Schwann cell as the tumor-initiating cell. It is possible that neurofibroma formation results from the p75+/GFAP-negative cells in peripheral nerve, and/or that loss of *Nf1* within mature myelinating Schwann cells have non-cell autonomous effect(s) that promote tumor formation – similar to the non-cell autonomous effect on hematopoietic cells when *Nf1* is lost within stromal cells.

Perinatal tamoxifen injection into *PlpCre;Nf fl/fl* mice resulted in GEM grade I neurofibroma formation that resulted in morbidity at 15-23 months old. In contrast, adult loss of *Nf1* resulted in large neurofibromas which caused morbidity beginning 5 months post tamoxifen introduction. We considered the possibility that recombination occurs in more cells when tamoxifen-induced recombination occurs in adults. However, twice as many cells in sciatic nerve and three times as many in the DRG were EGFP+ in pups as compared to adult mice. Therefore together with previous studies showing that loss of *Nf1* in most developing Schwann cells leads to robust neurofibroma formation (22-24) we conclude that cells exist in the adult peripheral nervous system that remain susceptible to neurofibroma formation, and that the susceptible population(s) may be enriched in adult and embryonic nervous systems.

Le et al's co-submitted study confirms our observation that neurofibromas can form after perinatal or adult loss of *Nf1*. However, while they identified small neurofibromas at the thoracic and lumbo-sacral levels after adult loss of *Nf1*, we generated large neurofibromas throughout the neuroaxis. Some differences between the two studies may account for the slightly different findings. Lu et al. provided 4 mg tamoxifen (2mg twice daily) by oral gavage to adult mice for 5 days, while we dosed 1mg twice day by I.P. injection for 3 days. It is also possible that the different phenotypes result from the different tamoxifen-inducible *PlpCre* driver lines used in the two studies. This difference may well account for the absence of hematopoietic lesions in their system. Most importantly, our data do not support the idea that there is a critical window for neurofibroma formation.

Mast cells, and other hematopoietic cells, showed <1% recombination in *PlpCre;Nf1fl/fl* mice, yet neurofibroma formation was robust. While *Krox20Cre;Nf1fl/fl* mice show hyperplasia within the DRG, neurofibroma development required an $Nf1^{+/-}$ background attributed to $Nf1^{+/-}$ mast cells (22, 35). *DhhCre;Nf1fl/fl* animals develop neurofibromas when only Schwann cell lineage cells are *Nf1* mutant (24), and the *PlpCre;Nf1fl/fl* model is similar in that a heterozygous background is not necessary for neurofibroma formation.

The peripheral blood of *PlpCre;Nf1fl/fl* mice showed a decrease in monocytes with a relative increase in lymphocytes and PMN. In contrast, *Nf1* loss driven by Mx1-Cre causes a mouse disorder similar to human juvenile myelomonocytic leukemia (JMML), with hyperproliferation of all hematopoietic cell types and progressive myeloproliferative disorder (36, 37, 38). Flow cytometry and immunohistochemistry showed that the *PlpCre* transgene did not cause *Nf1* loss in cells of hematopoietic origin. Rather, EGFP+ cells within these tumors had a stromal/mesenchymal appearance, and some double-labeled with Sca-1. EGFP expression did not co-localize with the expression of hematopoietic lineage markers or c-kit (data not shown), indicating that recombined EGFP+ cells had a non-hematopoietic, mesenchymal origin (30, 39).

The idea that *Nf1* loss can affect tumorigenesis in a non-cell autonomous fashion (e.g. myelinating cells acting upon other cells in the nerve) is thus supported by analogy to the

formation of hematopoietic lesions within the *PlpCre;Nf1fl/fl* animals, in which mutant stromal cells after either perinatal or adult tamoxifen-induced *Nf1* loss, cause lymphoid and myeloid proliferation. However we cannot exclude the possibility that neurofibroma formation requires *Nf1* loss of function in a small population of stem/progenitor-like cells that remain unidentified by our analysis, or induces expression of chemoattractants that result in massive tissue infiltration by hematopoietic cells. In either event, neurofibroma formation is not restricted to loss of *Nf1* in embryonic life, but can be triggered by *Nf1* loss throughout life.

Supplementary Material

Refer to Web version on PubMed Central for supplementary material.

Acknowledgments

We thank Brian Popko (University of Chicago) for providing the inducible Plp-Cre-ERT mice. The DAMD Program on Neurofibromatosis (W81XWH-06-1-0114 to T.A.R. and N.R.) *and NIH R01-NS28840 (NR) supported this work*. NIH NRSA (T32CA117846) and National Multiple Sclerosis Society (FG1762A1/1) supported D.A.M.

References

1. Friedman JM. Epidemiology of neurofibromatosis type 1. Am J Med Genet. 1999; 891:1–6. [PubMed: 10469430]
2. Boyd KP, Korf BR, Theos A. Neurofibromatosis type 1. J Am Acad Dermatol. 2009; 611:1–14. [PubMed: 19539839]
3. Rosenfeld A, Listernick R, Charrow J, Goldman S. Neurofibromatosis type 1 and high-grade tumors of the central nervous system. Childs Nerv Syst. 2010; 265:663–7. [PubMed: 19937438]
4. Emanuel PD, Bates LJ, Castleberry RP, et al. Selective hypersensitivity to granulocyte-macrophage colony-stimulating factor by juvenile chronic myeloid leukemia hematopoietic progenitors. Blood. 1991; 77:925–929. [PubMed: 1704804]
5. Niemeyer CM, Arico M, Basso G, et al. Quantitative effects of Nf1 inactivation on in vivo hematopoiesis. Blood. 1997; 89:3534. [PubMed: 9160658]
6. Side LE, Emanuel PD, Taylor B, et al. Mutations of the NF1 gene in children with juvenile myelomonocytic leukemia without clinical evidence of neurofibromatosis, type1. Blood. 1998; 92:267–272. [PubMed: 9639526]
7. Woodruff JM. Pathology of tumors of the peripheral nerve sheath in type 1 neurofibromatosis. Am J Med Genet. 1999; 891:23–30. [PubMed: 10469433]
8. Serra E, Puig S, Otero D, et al. Confirmation of a double-hit model for the NF1 gene in benign neurofibromas. Am J Hum Genet. 1997; 61:512–519. [PubMed: 9326316]
9. Serra E, Ars E, Ravella A, et al. Somatic NF1 mutational spectrum in benign neurofibromas; mRNA splice defects are common among point mutations. Human Genetics. 2001; 108:416–429. [PubMed: 11409870]
10. Maertens O, Brems H, Vandesompele J, et al. Comprehensive NF1 screening on cultured Schwann cells from neurofibromas. Hum Mutat. 2006; 27:1030–40. [PubMed: 16941471]
11. Dong Z, Sinanan A, Parkinson D, et al. Schwann cell development in embryonic mouse nerves. J Neuroscience Research. 1999; 56:334–348.
12. Jessen KR, Mirsky R. The origin and development of glial cells in peripheral nerves. Nature Reviews. 2005; 6:671–682.
13. Bixby S, Kruger GM, Mosher JT, et al. Cell-intrinsic differences between stem cells from different regions of the peripheral nervous system regulate the generation of neural diversity. Neuron. 2002; 35:643–656. [PubMed: 12194865]
14. Joseph NM, Mosher JT, Buchstaller J, et al. The loss of Nf1 transiently promotes self-renewal but not tumorigenesis by neural crest stem cells. Cancer Cell. 2008; 132:129–40. [PubMed: 18242513]

15. Kleber M, Lee HY, Wurdak H, et al. Neural crest stem cell maintenance by combinatorial Wnt and BMP signaling. The Journal of Cell Biology. 2005; 169:309–320. [PubMed: 15837799]
16. Morrison SJ, White PM, Zock C, Anderson DJ. Prospective identification, isolation by flow cytometry, and in vivo self-renewal of multipotent mammalian neural crest stem cells. Cell. 1999; 965:737–49. [PubMed: 10089888]
17. Nagoshi N, Nagoshi N, Shibata S, et al. Ontogeny and multipotency of neural crest-derived stem cells in mouse bone marrow, dorsal root ganglia, and whisker pad Cell. Stem Cell. 2008; 2:392–403.
18. Mirsky R, Woodhoo A, Parkinson DB, et al. Novel signals controlling embryonic Schwann cell development, myelination and dedifferentiation. J Peripheral Nervous System. 2008; 13:122–135.
19. Brannan CI, Perkins AS, Vogel KS, et al. Targeted disruption of the neurofibromatosis type-1 gene leads to developmental abnormalities in heart and various neural crest-derived tissues. Genes & Development. 1994; 8:1019–1029. [PubMed: 7926784]
20. Jacks T, Shih TS, Schmitt EM, Bronson RT, Bernards A, Weinberg RA. Tumour predisposition in mice heterozygous for a targeted mutation in Nf1. Nat Genet. 1994; 7:353–361. [PubMed: 7920653]
21. Gitler AD, Zhu Y, Ismat FA, et al. Nf1 has an essential role in endothelial cells. Nat Genet. 2003; 331:75–9. [PubMed: 12469121]
22. Zhu Y, Ghosh P, Charnay P, et al. Neurofibromas in NF1; Schwann cell origin and role of tumor environment. Science. 2002; 296:920–922. [PubMed: 11988578]
23. Zheng H, Chang L, Patel N, et al. Induction of abnormal proliferation by nonmyelinating Schwann cells triggers neurofibroma formation. Cancer Cell. 2008; 13:117–128. [PubMed: 18242512]
24. Wu J, Williams JP, Rizvi TA, et al. Plexiform and dermal neurofibromas and pigmentation are caused by Nf1 loss in desert hedgehog-expressing cells. Cancer Cell. 2008; 13:105–116. [PubMed: 18242511]
25. Mallon BS, Shick HE, Kidd GJ, Macklin WB. Proteolipid Promoter Activity Distinguishes Two Populations of NG2-Positive Cells throughout Neonatal Cortical Development. J Neuroscience. 2002; 22(3):876–885.
26. Doerflinger NH, Macklin WB, Popko B. Inducible site-specific recombination in myelinating cells. Genesis. 2003; 35:63–72. [PubMed: 12481300]
27. Nakamura T, Colbert MC, Robbins J. Neural crest cells retain multipotential characteristics in the developing valves and label the cardiac conduction system. Circ Res. 2006; 9812:1547–54. [PubMed: 16709902]
28. Stemmer-Rachamimov AO, Louis DN, Nielsen GP, et al. Comparative pathology of nerve sheath tumors in mouse models and humans. Cancer Res. 2004; 64(10):3718–24. [PubMed: 15150133]
29. Feng JM, Fernandes AO, Bongarzone ER, et al. Expression of soma-restricted proteolipid/DM20 proteins in lymphoid cells. J Neuroimmunology. 2003; 144:9–15. [PubMed: 14597093]
30. Morikawa S, Mabuchi Y, Kubota Y, et al. Prospective identification, isolation, and systemic transplantation of multipotent mesenchymal stem cells in murine bone marrow. J Exp Med. 2009; 20611:2483–96. [PubMed: 19841085]
31. Gao J, Yan XL, Li R, et al. Characterization of OP9 as authentic mesenchymal stem cell line. J Genet Genomics. 2010; 377:475–82. [PubMed: 20659712]
32. Peister A, Mellad JA, Larson BL, et al. Adult stem cells from bone marrow MSCs isolated from different strains of inbred mice vary in surface epitopes, rates of proliferation, and differentiation potential. Blood. 2004; 103:1662–1668. [PubMed: 14592819]
33. Gupta SK, Pringle J, Poduslo JF, Mezei C. Levels of proteolipid protein mRNAs in peripheral nerve are not under stringent axonal control. J Neurochem. 1991; 56(5):1754–62. [PubMed: 1707441]
34. Ling BC, Wu J, Miller SJ, et al. Role for the epidermal growth factor receptor in neurofibromatosis-related peripheral nerve tumorigenesis. Cancer Cell. 2005; 71:65–75. [PubMed: 15652750]
35. Yang FC, Ingram DA, Chen S, et al. Nf1-deficient tumors require a microenvironment containing Nf1+/−and c-kit-dependent bond marrow. Cell. 2008; 1353:437–448. [PubMed: 18984156]

36. Le DT, Kong N, Zhu Y, et al. Somatic inactivation of Nf1 in hematopoietic cells results in a progressive myeloproliferative disorder. Blood. 2004; 103:4243–4250. [PubMed: 14982883]

37. Zhang Y, Taylor BR, Shannon K, Clapp DW. Defective proliferative responses in B lymphocytes and thymocytes that lack neurofibromin. J Clin Invest. 2001; 1085:709–15. [PubMed: 11544276]

38. Kim TJ, Cariappa A, Iacomini J, et al. Defective proliferative responses in B lymphocytes and thymocytes that lack neurofibromin. Mol Immunol. 2002; 389:701–8. [PubMed: 11858825]

39. Chan CK, Chen CC, Luppen CA, et al. Endochondral ossification is required for haematopoietic stem-cell niche formation. Nature. 2009; 457(7228):490–4. [PubMed: 19078959]

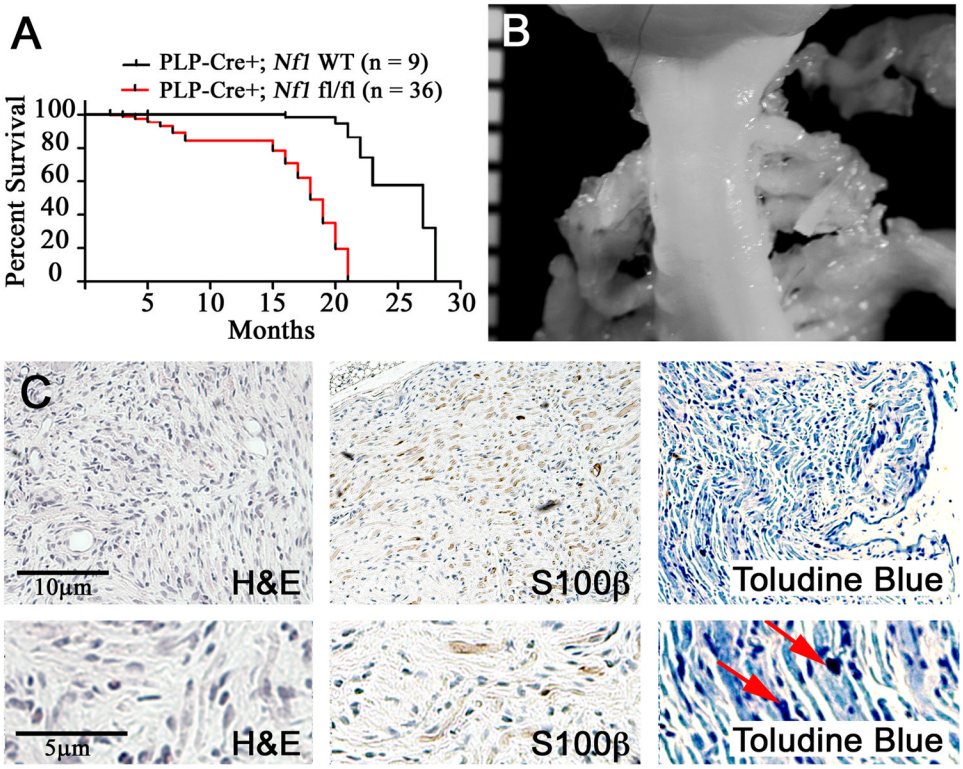

Figure 1. Perinatal loss of *Nf1* mice causes two phases of mortality and late neurofibroma formation

(A) Kaplan-Meyer survival curve ($p < 0.0001$). (B) Gross dissection of cervical spinal cord with DRG-associated small GEM Grade I neurofibromas at each dorsal root in a *PlpCre+;Nf1fl/fl* animal at 18 months of age. Ruler shows 1mm markings. (C) Tissue sections of GEM Grade I neurofibroma in *PlpCre+;Nf1fl/fl* animal after perinatal tamoxifen. Upper panels are magnified 10×; lower panels 25×. Red arrows highlight mast cells.

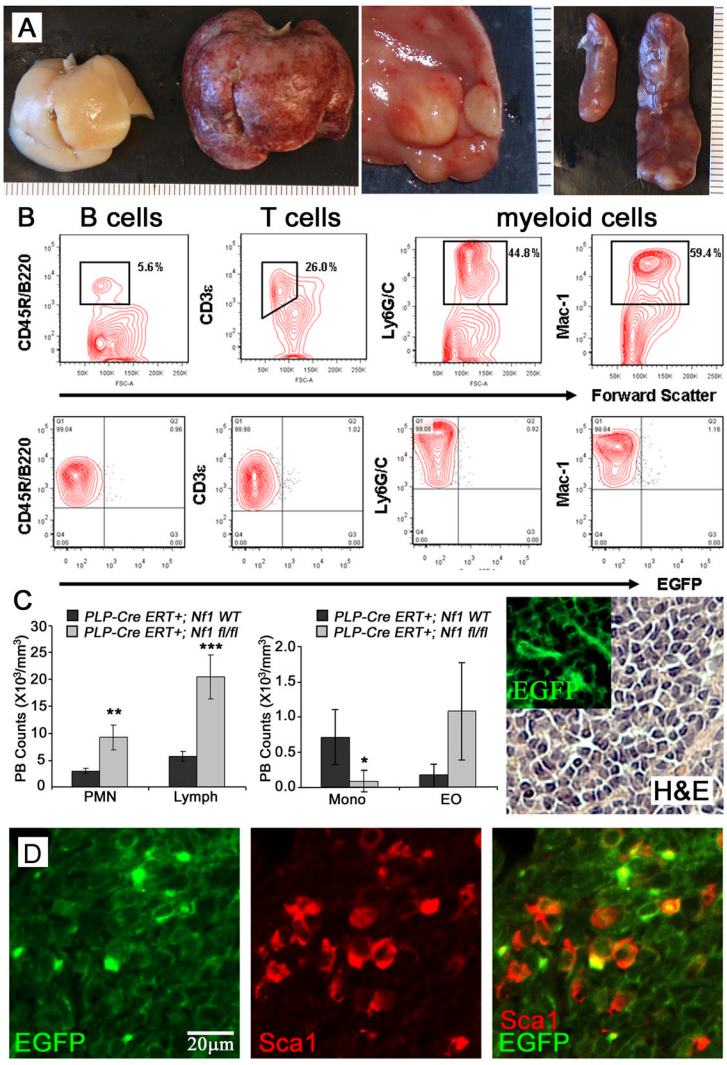

Figure 2. Perinatal *Nf1* loss causes reactive hyperplasia of hematopoietic cells

(A) Left, wild type liver; Middle, *Nf1fl/fl* enlarged liver with white masses; Right, enlarged *Nf1fl/fl* spleen with white masses (right) compared to a wildtype spleen (left). Rulers show 1mm markings. (B) Flow cytometric analysis of splenocytes from *PLP-Cre ERT+;Nf1fl/fl;EGFP+* mice, analyzed for content of B (CD45R/B220), T (CD3e) and myeloid cells (Ly6G/C and Mac-1). All were EGFP-. (C). Peripheral blood counts from total CBC and Blood Smear Counts show increased PMN (** p = 0.0026) and lymphocytes (LY; *** p = 0.0006), and decreased monocytes (MO; * p = 0.0347) of *PLP-CreERT+;Nf1fl/fl* animals compared to age-matched litermate controls but not eosiniphils (EO). (C, right panel) H&E stain and EGFP+ (insert) cells within a liver mass. Insert and H&E are at the same magnification (40×). (D) Double labeled Sca1+ (red) and EGFP+ (green) cells (40×). Round cells of possible lympho-hematopoietic lineage are EGFP negative.

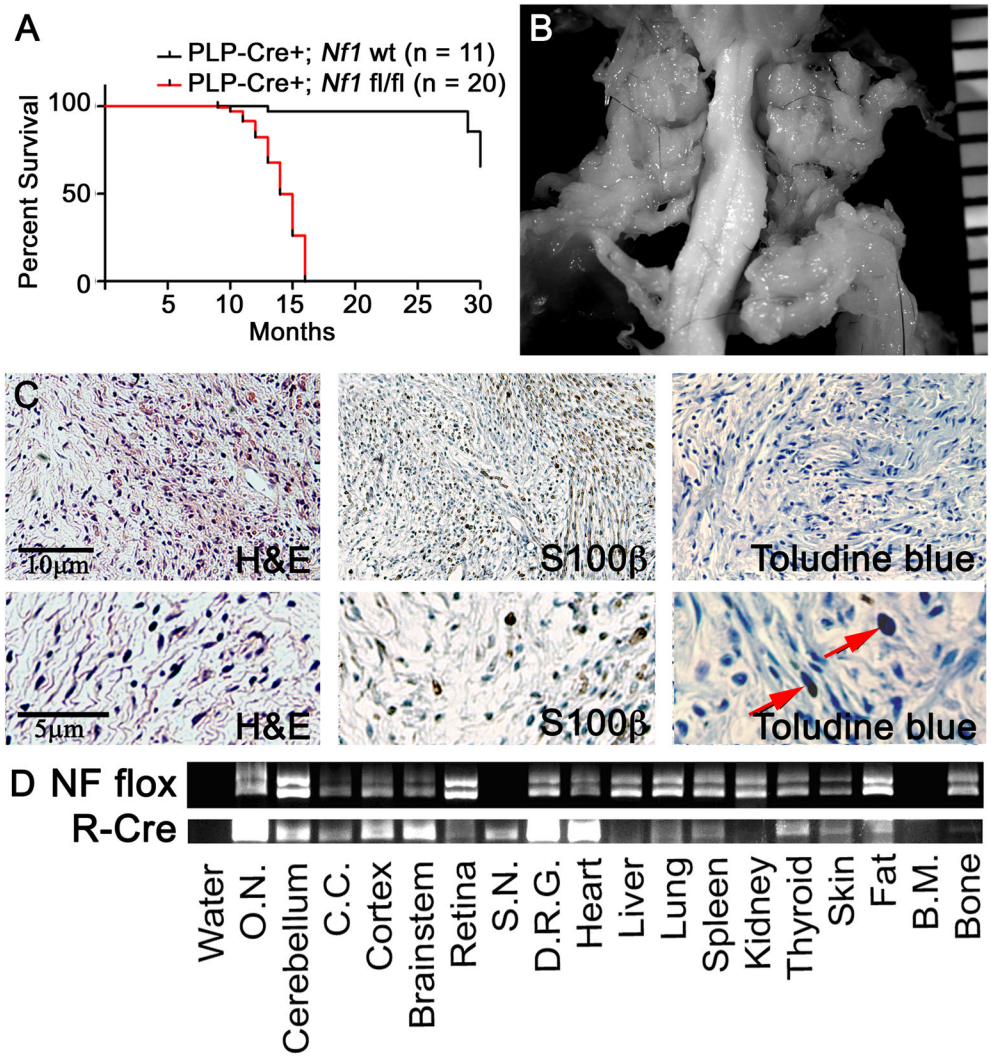

Figure 3. Adult Tamoxifen exposure in *PlpCre;Nf1fl/fl* mice causes neurofibroma formation

(A) Kaplan-Meyer survival curve ($p < 0.0001$). (B) Gross dissection of cervical spinal cord with GEM Grade I neurofibromas in a *PlpCre+;Nf1fl/fl* animal. Ruler shows 1mm markings. (C) Tissue sections of a GEM Grade I neurofibroma in a *PlpCre+;Nf1fl/fl* animal after adult tamoxifen. Upper panels are magnified 10×; lower panels are magnified 25×. Red arrows highlight mast cells. (D) PCR analysis shows the Nf1 floxed allele (NF flox) and the recombined Cre allele (R-Cre). Each lane contains 1ug of DNA. (O.N. = optic nerve; C.C. = corpus callosum; S.N. = sciatic nerve; DRG = dorsal root ganglia; B.M. = bone marrow).

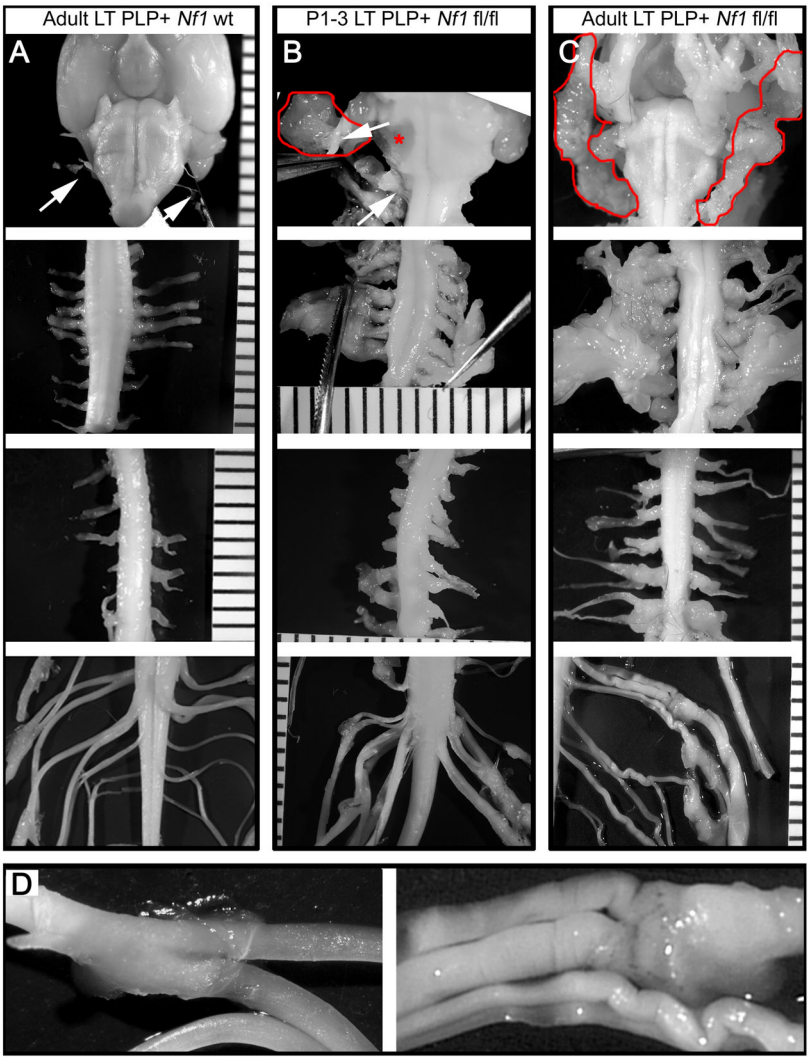

Figure 4. Neurofibroma formation is predominant within the peripheral nerves and DRGs at cervical spinal levels

Gross micrographs show age-matched 12 month old (A) *PlpCre;WT*, (B) P1-3 tamoxifen-injected *PlpCre;Nf1fl/fl*, and (C) adult tamoxifen-injected *PlpCre;Nf1fl/fl* animals. Brainstem (top row), cervical (second row), thoracic (third row), and lumbar/sacral (forth row) spinal cord. Ruler shows 1mm markings. Arrows (A & B) = cranial nerves emerging from the brainstem. Red lines (B & C) = facial neurofibromas developed from cranial nerves. Red asterisk (* in B) = compression of the brainstem resulting from cranial nerve neurofibroma (pulled away with forceps to show compression). In cervical neurofibroma images (B & C; second row) forceps slightly pulled the nerves from the spinal cord to visualize tumors. Adult tamoxifen-injected *PlpCre;*WT and *PlpCre;Nf1fl/fl* peripheral nerves of the cauda equine are shown enlarged in D.

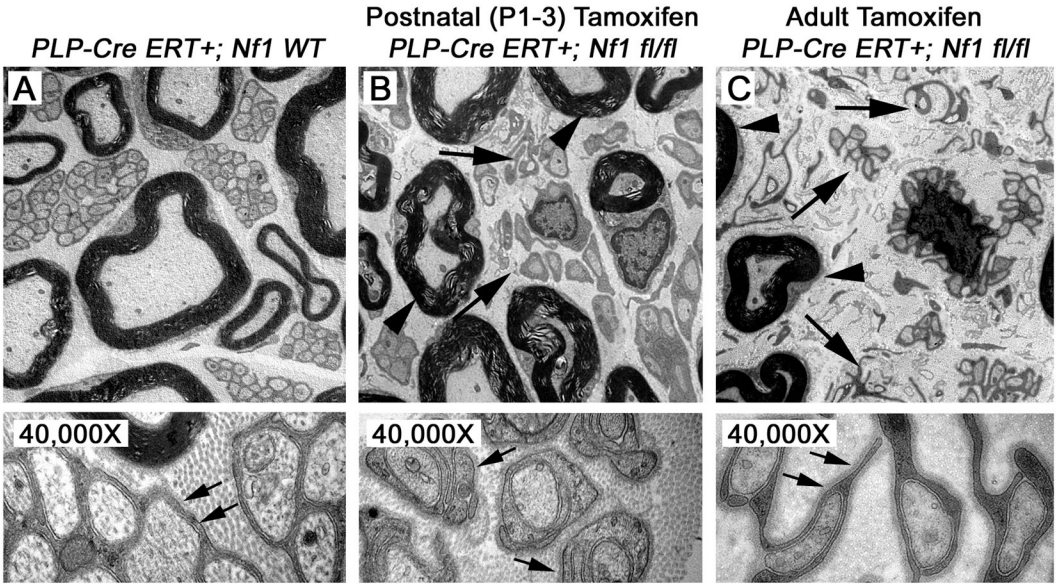

Figure 5. Disrupted Remak bundles in *PlpCre;Nf1fl/fl* nerves

Electron micrographs of the saphenous nerves of 12 month old (A) *PlpCre+;WT* control, (B) P1-3 tamoxifen-injected *PlpCre+;Nf1fl/fl*, and (C) adult tamoxifen-injected *PlpCre+;Nf1fl/fl* animals. Large Arrows in B & C highlight Remak bundle disruption; arrowheads highlight myelin sheaths in B & C. 4,000× = upper panels. 40,000× = lower panels. Schwann cell cytoplasmic processes are identified by their continuous basal lamina (small arrows lower panels).

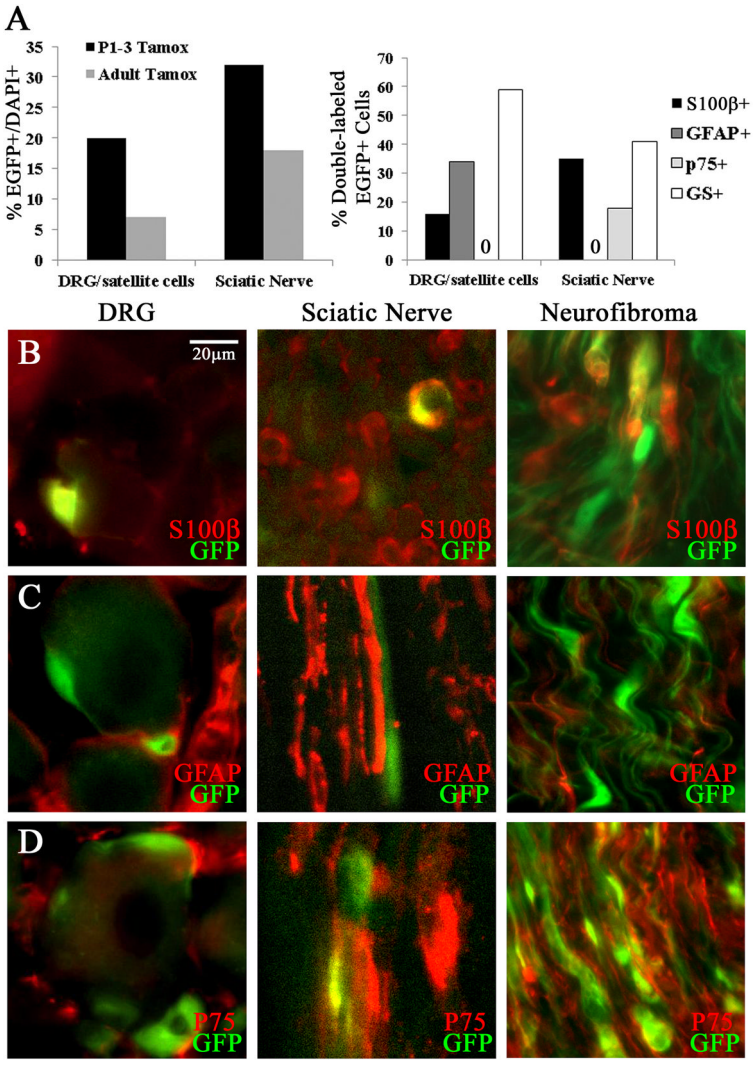

Figure 6. EGFP+ cells after tamoxifen injection in *PlpCre*+ animals

(A) Graph (left) indicates percentages of EGFP+/DAPI+ cells in sciatic nerve and DRG/satellite cells and (right) the percent of EGFP+ recombined cells that double labeled with S100β, GFAP, p75, or GS. (B) Double immunolabeling (40×) shows EGFP+/S100β+ cells within the DRG or Sciatic Nerve one day post Tamoxifen. (C) EGFP+/GFAP+ cells are present in the DRG but not Sciatic Nerve. (D) EGFP+/p75+ cells are absent in the DRG and present in Sciatic Nerve. Immunohistochemistry in neurofibromas after adult tamoxifen exposure within the *PlpCre;Nf1fl/fl* model shows EGFP double labeling with S100β+ (B), p75 (D) but not GFAP+ (C).

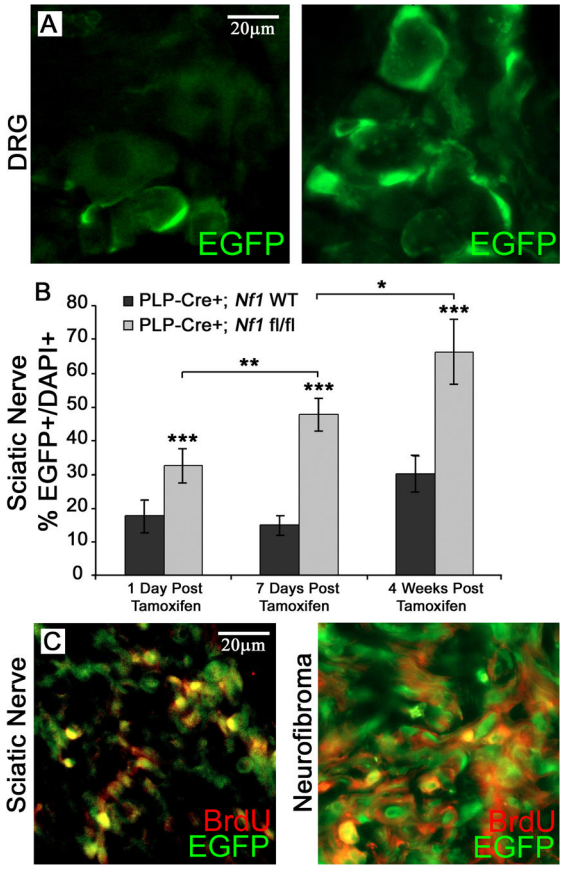

Figure 7. EGFP+ cells proliferate in *PlpCre*+ animals

EGFP+ cells (green; 40×) within the DRG one day post last Tamoxifen injection (A, left) and 15 months post Tamoxifen (A, right) in *PlpCre;Nf1fl/fl* animals. (B) Quantification of the EGFP+ population in sciatic nerves of *PlpCre;Nf1fl/fl* and littermate wild type animals (n = 3-5 per time point per genotype). The total % EGFP+/DAPI+ cells were calculated after times after tamoxifen injection. BrdU immunostaining (40×) co-localizes in EGFP+ cells at 4 weeks post Tamoxifen injection (C, left) and within a neurofibroma (C, right). ***** $p < 0.01$; ****** $p < 0.001$; ******* $p < 0.00001$.